Bioorganic & Medicinal Chemistry Letters 18 (2008) 6369–6373

Contents lists available at ScienceDirect

Bioorganic & Medicinal Chemistry Letters

journal homepage: www.elsevier.com/locate/bmcl

The discovery of AZD5597, a potent imidazole pyrimidine amide CDK inhibitor suitable for intravenous dosing

Clifford D. Jones [a,*], David M. Andrews [a], Andrew J. Barker [a], Kevin Blades [a], Paula Daunt [a], Simon East [a], Catherine Geh [a], Mark A. Graham [a], Keith M. Johnson [a], Sarah A. Loddick [a], Heather M. McFarland [a], Alexandra McGregor [a], Louise Moss [a], David A. Rudge [a], Peter B. Simpson [a], Michael L. Swain [a], Kin Y. Tam [a], Julie A. Tucker [b], Mike Walker [a]

[a] Cancer and Infection Research, AstraZeneca Pharmaceuticals, Alderley Park, Macclesfield, Cheshire SK10 4TG, UK
[b] Lead Generation-Discovery Enabling Capabilities and Sciences, AstraZeneca Pharmaceuticals, Alderley Park, Macclesfield, Cheshire SK10 4TG, UK

ARTICLE INFO

Article history:
Received 20 August 2008
Revised 17 October 2008
Accepted 18 October 2008
Available online 25 October 2008

Keywords:
Kinase
Cyclin-dependent kinase
Kinase inhibitor
Imidazole amide
CDK
Cell cycle
Anti-cancer

ABSTRACT

The development of a novel series of imidazole pyrimidine amides as cyclin-dependent kinase (CDK) inhibitors is described. Optimisation of inhibitory potency against multiple CDK's (1, 2 and 9) resulted in imidazole pyrimidine amides with potent in vitro anti-proliferative effects against a range of cancer cell lines. Excellent physiochemical properties and large margins against inhibition of CYP isoforms and the hERG ion channel were achieved by modification of lipophilicity and amine basicity. A candidate with disease model activity in human cancer cell line xenografts and with suitable physiochemical and pharmacokinetic profiles for intravenous (iv) dosing was selected for further development as AZD5597.

The cyclin-dependent kinase (CDK) family are two groups of serine–threonine protein kinases with roles in the coordination of the eukaryotic cell cycle and transcriptional regulation. Because of their critical role in the regulation of the cell cycle and the observed expression/activity pattern in most human cancers, considerable effort has been focused on the development of small molecule CDK cell cycle inhibitors as potential therapeutic agents.[1]

Recently, the observation of functional redundancy within the CDK family has led to the belief that inhibitors that are highly selective for individual CDKs may not be therapeutically effective. The best combination of CDK activities that will lead to the greatest efficacy with minimal toxicity is still under debate. It is known that combined depletion of CDK1 and CDK2 is more pro-apoptotic than depletion of either CDK alone, and that CDK1 inhibition leads to MYC-dependent apoptosis.[2,3] In addition, the roles of the non-cell cycle CDKs such as CDK7 and CDK9 in transcriptional regulation is now better understood. The clinical activity observed in chronic lymphocytic leukaemia with the CDK inhibitor flavopiridol may be partly accounted for by the inhibition of CDK9 leading to apoptosis. Since clinical responses would be preferable to stable disease then a pro-apoptotic rather than a cytostatic agent could be optimal. Consequently, agents which inhibit the function of multiple CDKs may be clinically more successful than very selective CDK inhibitors.[4]

Our previous efforts to discover novel CDK inhibitors led to the identification of the imidazole sulfone AZD5438 (**1**) that was investigated further as an orally bioavailable anti-cancer agent (Fig. 1).[5] Replacement of the sulfone with piperazine led to a new series of potent CDK inhibitors (**2**) with improved physical properties that were also suitable for oral dosing.[6] To complement these compounds, we next sought to obtain a CDK inhibitor with properties that allowed dosing as an iv agent. In addition, the emerging

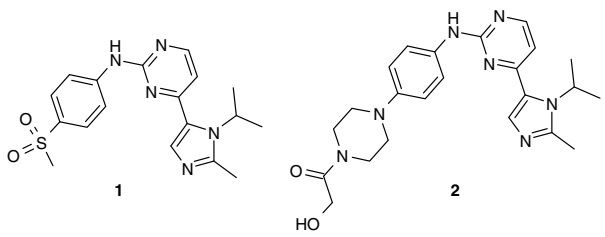

Figure 1. Astrazeneca CDK inhibitors AZD5438 (**1**) and piperazine (**2**).

* Corresponding author. Tel.: +44 1625 513670.
E-mail address: cliff.jones@astrazeneca.com (C.D. Jones).

0960-894X/$ - see front matter © 2008 Elsevier Ltd. All rights reserved.
doi:10.1016/j.bmcl.2008.10.102

information concerning CDK function led us to choose to target the inhibition of CDK1, 2 and 9.

As well as obtaining a suitable CDK profile, a number of physiochemical properties also need to be under close control in order to obtain an agent suitable for iv dosing. These properties include excellent solubility and extended stability of the formulated drug to chemical, enzymatic or photolytic degradation. Acquired long QT syndrome is a major problem in clinical studies due to the occurrence of significant cardiac side effects. Inhibition of the human ether-a-go-go-related-gene (hERG) potassium ion channel can lead to the development of arrhythmias related to long QT. As short infusions or iv bolus doses generally lead to high maximum concentrations of free drug (free C_{max}) we sought to avoid significant hERG inhibition by early screening using a high-throughput patch–clamp hERG assay.[7] This paper describes the identification, development and synthesis of a new chemical series with CDK inhibitory profiles and physiochemical properties suitable for iv dosing.

We hypothesized that incorporation of a basic group into our CDK imidazole pyrimidine amide inhibitor series offered the best opportunity to achieve the required properties. The route developed to obtain these compounds is shown in Scheme 1. The synthesis of the aminopyrimidines (**3**, R^1 = H or F) has been reported previously.[6,8] Palladium catalysed coupling with ethyl 4-iodobenzoate followed by hydrolysis gave the corresponding acids **4**. These acid intermediates were subject to late stage diversification by coupling with amines to give the amides (**5a**–**12a** and **5b**–**12b**). Alternatively, for larger scale work it proved more convenient to couple the 4-iodoarylamides directly with the aminopyrimidines **3** using palladium catalysis. The 4-iodoarylamides were readily obtained by reaction of the required amine with 4-iodobenzoyl chloride. Similar routes using 4-bromo-2-fluoroarylamides were used to obtain the ortho-fluoro substituted amides (**6c,d** and **7c,d**). The 4-bromo-2-fluoroarylamides were obtained by reacting the corresponding acid under standard amide coupling conditions (HATU, NEt_3, DMF) with the requisite amine.

An initial set of piperazine amides were synthesised using these routes and compared with our first clinical candidate, the orally bioavailable CDK inhibitor AZD5438 **1** (Table 1). The 5-H pyrimidine piperazine amide **5a** possessed a similar enzyme and cellular

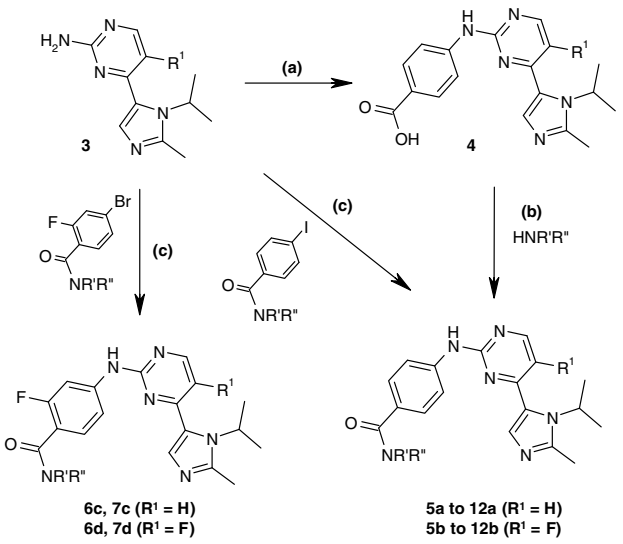

Scheme 1. Synthesis of imidazole amides. Reagents (a) i—ethyl4-iodobenzoate, $Pd(OAc)_2$, Xantphos, Cs_2CO_3, 1,4-dioxane, 32–67%; ii—NaOH, THF/water, 94%; (b) HATU, DIPEA, DMF, 49%; (c) $Pd(OAc)_2$, Xantphos, Cs_2CO_3, 1,4-dioxane, 34–78%.

Table 1
CDK inhibition profile for compounds **5** and **6**.

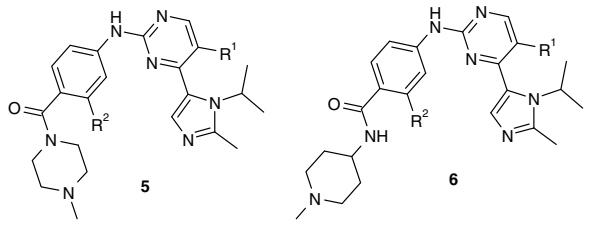

Compound	R^1	R^2	CDK2 IC_{50} (μM)	CDK1 IC_{50} (μM)	LoVo IC_{50}[a] (μM)	Solubility (μM)[b]
1	AZD5438		0.006	0.062	0.80	588[c]
5a	H	H	0.009	0.071	0.52	480
5b	F	H	0.018	0.13	0.17	60
6a	H	H	0.037	0.18	2.1	880
6b	F	H	0.036	0.05	0.32	>2500
6c	H	F	0.011	0.15	0.20	>2200
6d	F	F	0.001	0.012	0.08	270

[a] IC_{50} for inhibition of BrdU incorporation to LoVo cells following 48 h exposure to test compound.
[b] Equilibrium solubility measured over 24 h at pH 7.4.
[c] Mesylate salt.

profile to the previous clinical candidate. Whilst encouraging, the level of CDK1 potency needed further improvement, as we required an agent that was equipotent against CDK1 and CDK2. The potency benefits of 5-fluoro pyrimidine substitution in related chemical series have been discussed previously.[6,9] The increased lipophilicity of the 5-fluoro pyrimidine **5b** resulted in an improvement in cellular anti-proliferative potency due to increased cellular permeability, but was approximately 10-fold less potent against CDK1. The effect of the increased lipophilicity of **5b** was observed in the lower aqueous solubility compared to **5a**, which was not optimal for an iv agent. As the basicity of the piperazine amides is relatively low (measured pK_a 7.0 for **5a**), we expected that stronger bases would improve solubility, so the corresponding piperidine amides were synthesised in order to improve this key parameter.

Compared to the piperazine **5a**, the piperidine amide **6a** has lower enzyme potency along with lower levels of cellular anti-proliferative activity. The CDK2 enzyme potency of the 5-fluoro-pyrimidine equivalent **6b** was similar to **6a** and the overall enzyme profile was more promising as, for the first time, we observed near equipotency for CDK2 and CDK1. We were also encouraged to observe the large solubility benefit of the piperidine (measured pK_a 8.8 for **6d**) compared to the less basic piperazine **5a**.

Fluorine substitution adjacent to a secondary amide was shown to be beneficial for potency in an earlier alkyl amide series.[8] This was observed again, with an encouraging increase in potency for the ortho-fluoro substituted amide **6c** compared to the unsubstituted **6a**. Combining both beneficial changes in the ortho-fluoro substituted, 5-fluoro pyrimidine **6d** resulted in an extremely promising profile with good levels of CDK1 and CDK2 enzyme potency which translated into excellent levels of anti-proliferative cellular activity. The decrease in solubility of **6d** compared to **6b** was due to a combination of increased lipophilicity and the presence of an internal NH–F hydrogen bond. This bond results in a more planar structure leading to improved packing in the solid state and lower solubility. Encouraged by the overall favourable profile of **6d** we decided to focus on exploring a range of other amides linked to basic functionality (Table 2).

Table 2
CDK inhibition profile for compounds **7**, **8** and **9**.

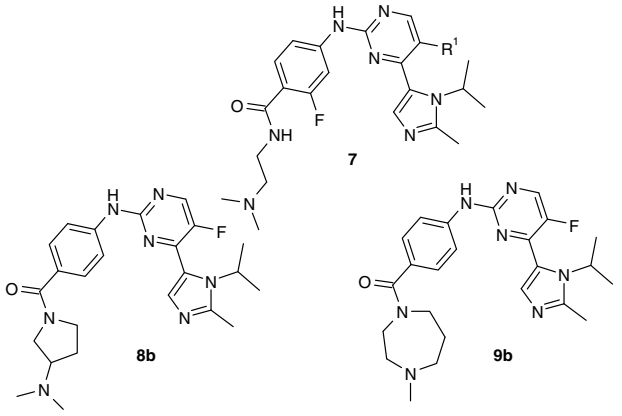

Compound	R^1	CDK2 IC_{50} (μM)	CDK1 IC_{50} (μM)	LoVo IC_{50} (μM)	Solubility (μM)
7c	H	0.003	0.029	0.003	>1900
7d	F	0.002	<0.001	0.002	>2700
(*S*)-**8b**	F	0.002	0.011	0.037	>2100
(*R*)-**8b**	F	0.006	0.011	0.070	>2400
9b	F	0.002	0.005	0.040	>2600

In addition to excellent levels of enzyme and cellular anti-proliferative potency for a range of amide substituents, we also observed excellent levels of solubility. Again, for secondary amides, the 5-fluoro pyrimidine ortho-fluoro amide substitution pattern led to the highest levels of enzyme potency against both CDK1 and CDK2 (e.g., compare **7c** with **7d**). This highly potent CDK1/2 inhibition resulted in extremely potent inhibition of cellular proliferation in cancer cell lines. The chiral, non-racemic pyrrolidines ((*S*)-**8b**, (*R*)-**8b**) also displayed excellent potency against CDK1 and CDK2, again with potent anti-proliferative activity. In contrast to the piperazine amides (Table 1, **5b**), the corresponding homopiperazine **9b** gave much improved properties with significant increases in both enzyme and cellular potency. The increased basicity of the homopiperazine (measured pK_a 8.1 for **9b**) compared to the piperazine **5b** (measured pK_a 6.9) also resulted in much improved solubility (greater than the maximum value measurable in this assay).

Additional profiling of a selection of these compounds demonstrated the attractiveness of the 5-fluoro amide series as potential iv agents (Table 3). All the compounds showed good levels of CDK9 inhibition, particularly the dimethylethylamino amide **7d** and the pyrrolidine (*S*)-**8b**. The high levels of CDK9 potency, along with potent inhibition of CDK1/2, leads to apoptosis in proliferating cancer cells and is responsible for the unprecedented levels of anti-proliferative activity of these compounds. The compounds tested also had an attractive balance of lipophilicity with excellent physical properties. The lack of significant hERG activity would avoid inhibition of the hERG channel during the high free C_{max} levels achieved in iv bolus dosing or short duration infusions.

Rat iv pharmacokinetic studies showed that the compounds had a range of clearances in the low to moderate range. The volume of distribution varied from high to moderate depending on the pK_a of the amine. We felt that all the compounds had favourable profiles as iv agents but as the pyrrolidine series had the best overall profile, it was selected for further progression.

The binding mode of the pyrrolidine series was confirmed by obtaining an X-ray crystal structure of (*S*)-**8b** bound to CDK2 (Fig. 2).

The electron density for the bound inhibitor is clearly defined.[16] Two hydrogen bonds are made from the aminopyrimidine to the backbone of the hinge residue, Leu83. The carbonyl group of the amide linkage makes an interaction with the backbone NH of Asp86, whilst the side-chain carboxylate of Asp86 contacts the nitrogen of the dimethylamine. This latter interaction probably accounts for the greater potency observed for the (*S*)-enantiomer (*S*)-**8b** over the (*R*)-enantiomer (*R*)-**8b**.

The attractive profile of the pyrrolidine series led us to further explore variation of the substituents on the pyrrolidine ring using the route shown in Scheme 2. Commercially available (*R*)-3-hydroxypyrrolidine was coupled with 4-iodobenzoyl chloride (**10**) then activated as the methanesulfonyl ester (**11**). Displacement with inversion of stereochemistry occurred smoothly with a range of primary and secondary amines to give the (*S*)-4-iodoarylamide coupling partners (**12**). Subsequent coupling with the appropriate aminopyrimidine under Buchwald–Hartwig conditions as described in Scheme 1, gave the chiral, non-racemic pyrrolidine products in good yield.

Overall, potency against CDK2 was generally retained with a variety of amine substituents, however, CDK1 potency was more sensitive to substitution. This is illustrated by increasing the size of the amine substituent (e.g., in (*S*)-**13a**), where a good level of CDK2 potency was maintained but lower CDK1 activity was observed. A similar profile was seen with larger secondary amines (e.g., (*S*)-**14a**), which also had lower levels of anti-proliferative activity (Table 4). We were surprised by the sensitivity of CDK1 potency to substitution in this position, as the amine is solvent exposed and there is high CDK1/CDK2 sequence homology in the region adjacent to the substituted pyrrolidine ring.

Much improved levels of potency against CDK1 were observed for (*S*)-3-methylamine pyrrolidines. Again, varying levels of anti-proliferative activity were seen with 5-fluoro versus 5-H pyrimidine substitution. Although the 5-H pyrimidine (*S*)-**15a** potently inhibited both CDK1 and CDK2 enzyme activity, lower levels of anti-proliferative cellular activity were observed.

The best balance of CDK1/2 enzyme and anti-proliferative activity was observed with the more lipophilic 5-fluoropyrimidine (*S*)-methylamine, (*S*)-**15b**. With high levels of both enzyme potency and cellular anti-proliferative activity, this promising compound was progressed into additional physiochemical assays (Table 5).

The overall profile of (*S*)-**15b** indicated that it was suitable for further development as an iv agent. The high margins against hERG allow for flexibility in dosing either as a bolus or by extended infusions. The lack of CYP inhibition lowers the risk of problematic drug–drug interactions in the clinic. Excellent aqueous solubility from crystalline (*S*)-**15b** was obtained, even in simple saline for-

Table 3
Additional parameters for **6d**, **7d**, (*S*)-**8b** and **9d**.

Compound	CDK9 enzyme (μM)	log*D*	pK_a	Rat PPB (% free)	hERG (μM)	Dose (μmol/kg)	Rat Cl (mL/min/kg)	Vss (L/kg)	AUC (μM h)
6d	0.013	2.4	8.8	6	>32	2.5	16	5.2	1.3
7d	0.003	2.3	8.6	7	>65	2.5	24	9.8	0.8
(*S*)-**8b**	0.005	2.1	7.4[a]	4	33	2.5	23	3.4	0.8
9b	0.012	2.0	8.1	7	>32	1.0	28	1.5	0.3

[a] pK_a of racemate.

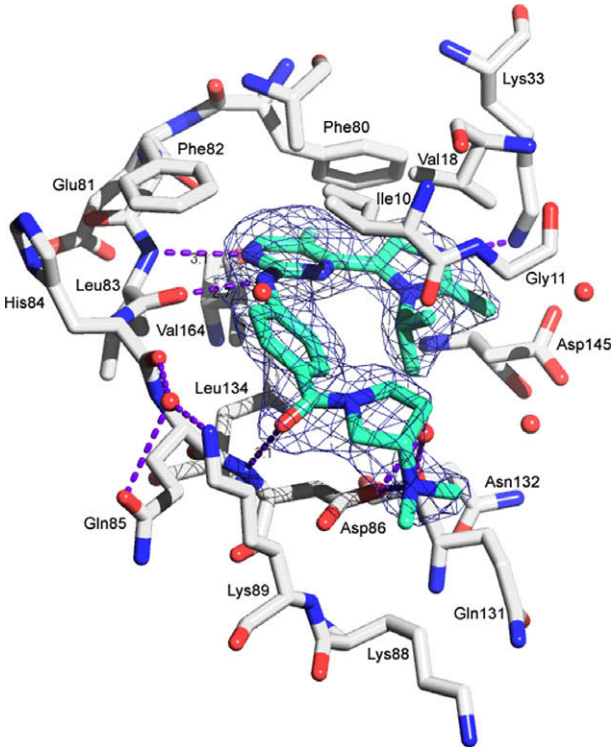

Figure 2. Crystal structure of (*S*)-**8b** bound to CDK2 showing final electron density for (*S*)-**8b** (blue 1.0σ level).[10] Figure was prepared using PyMol.[11]

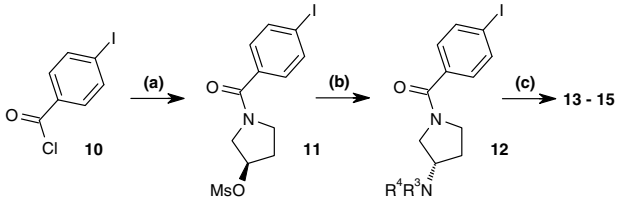

Scheme 2. Synthesis of (*S*)-pyrrolidine imidazole amides **13**–**15**. Reagents (a) (*R*)-3-hydroxypyrrolidine, Et_3N, CH_2Cl_2 then $MeSO_2Cl$, Et_3N, CH_2Cl_2 (81% over 2 steps); (b) amine, 1,4-dioxane, sealed tube (64–73%); (c) **3**, $Pd(OAc)_2$, Xantphos, Cs_2CO_3, 1,4-dioxane, 46–78%.

mulations. In addition, the formulated drug showed no significant decomposition on exposure to light, plasma or through chemical hydrolysis.

As well as these beneficial physiochemical properties, (*S*)-**15b** also possessed good pharmacokinetic parameters with moderate to low clearance in nude mouse and rat (Table 6). Clearance in the dog was higher (58% liver blood flow), due to the higher levels of free drug in dog plasma, but was still acceptable for an intravenously dosed drug.

Nude mice were implanted subcutaneously with SW620 human colon adenocarcinoma cells and in vivo tumour xenograft efficacy was established by dosing (*S*)-**15b** intraperitoneally (ip). Anti-tumour activity was observed with an inhibition of tumour volume of 55% ($P < 0.001$) when dosed intermittently (Monday, Wednesday, Friday) for 3 weeks at 15 mg/kg. On the basis of data presented, the compound (*S*)-**15b** was selected for further development as AZD5597.

In summary, we have discovered a new series of imidazole pyrimidine amides which possess excellent levels of anti-proliferative potency against cancer cell lines. Excellent physiochemical properties and large margins against inhibition of CYP isoforms and the hERG ion channel were also achieved. A lead compound, (*S*)-**15b** (AZD5597), was selected from the series for further development as a CDK inhibitor suitable for intravenous dosing.

Table 4
CDK inhibition profile for compounds **13**, **14** and **15**.

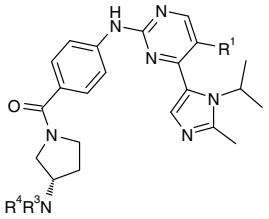

Compound	R^1	NR^3R^4	CDK2 IC_{50} (μM)	CDK1 IC_{50} (μM)	LoVo IC_{50} (μM)
(*S*)-**13a**	H	NMe^nPr	0.004	0.12	0.062
(*S*)-**14a**	H	NH^cPr	<0.001	0.10	0.25
(*S*)-**15a**	H	NHMe	0.002	0.009	0.18
(*S*)-**15b**	F	NHMe	0.002	0.002	0.039

Table 5
Additional data for (*S*)-**15b**.

Parameters	
log *D*	1.45
hERG (μM)	95
CYP inhibition[a] (μM)	All > 10
Aqueous solubility (mg/mL)[b]	>50
Photostability ($t_{1/2}$)	>24 h
Hydrolytic stability (pH 4–10) ($t_{1/2}$)	>100 days
Plasma stability[c]	>18 h

[a] Against Cyp isoforms: 3A4, 2D6, 2C9, 2C19, 1A2.
[b] At pH 5 in saline from crystalline (*S*)-**15b**.
[c] In rat, dog and human plasma.

Table 6
Pharmacokinetic parameters of (*S*)-**15b**.

PK parameters	Mouse[a]	Rat[b]	Dog[c]
PPB (% free)	16	4	>67
Dose (μmol/kg)	5.0	2.5	0.2
T½ (h)	3.4	3.6	32.3
Cl (mL/min/kg)	35	30	19
Vss (L/kg)	5.1	6.4	40.4
AUC (μM/h)	2.4	1.38	0.18

[a] Female nude.
[b] Male Han Wistar.
[c] Male Beagle.

Acknowledgments

We acknowledge the excellent technical expertise of the following scientists: Claire Brassington, Heather Haye, Eileen McCall and Sandra Oakes.

References and notes

1. Sharma, P. S.; Sharma, R.; Tyagi, R. *Curr. Cancer Drug Targets* **2008**, *8*, 53.
2. Cai, D.; Latham, V. M., Jr.; Zhang, X.; Shapiro, G. I. *Cancer Res.* **2006**, *18*, 9270.
3. Goga, A.; Yang, D.; Tward, A. D.; Morgan, D. O.; Bishop, J. M. *Nat. Med.* **2007**, *13*, 820.
4. Shapiro, G. I. *J. Clin. Oncol.* **2006**, *24*, 1770.
5. Anderson, M.; Andrews, D. M.; Barker, A. J.; Brassington, C. A.; Breed, J.; Byth, K. F.; Culshaw, J. D.; Finlay, M. R. V.; Fisher, E.; Gingell, H. H. J.; Green, C. P.; Heaton, D. W.; Nash, I. A.; Newcombe, N. J.; Oakes, S. E.; Pauptit, R. A.; Roberts, A.; Stanway, J. J.; Thomas, A. P.; Tucker, J. A.; Weir, H. M. *Bioorg. Med. Chem. Lett.* **2008**, *18*, 5487.

6. Finlay, M. R. V.; Acton, D. G.; Andrews, D. M.; Barker, A. J.; Dennis, M.; Fisher, E.; Graham, M. A.; Green, C. P.; Heaton, D. W.; Karoutchi, G.; Loddick, S. A.; Morgentin, R.; Roberts, A.; Tucker, J. A.; Weir, H. M. *Bioorg. Med. Chem. Lett.* **2008**, *18*, 4442.
7. Schroeder, K.; Neagle, B.; Trezise, DJ.; Worley, J. *J. Biomol. Screen.* **2003**, *8*, 50.
8. Andrews, D.; Finlay, M. R.; Green, C.; Jones, C. PCT Int. Application WO2006-064251.
9. Andrews, D. M.; Barker, A. J.; Blades, K.; Byth, K. F.; Finlay, M. R. V.; Geh, C.; Green, C. P.; Johannsen, M.; Jones, C. D.; Walker, M.; Weir, H. M. *Bioorg. Med. Chem. Lett.*, **2008**, doi:10.1016/j.bmcl.2008.10.075.
10. Protein and crystals were obtained according to established procedures.[12] Crystals were crosslinked with glutaraldehyde before soaking in 20 mM (*S*)-**8b** overnight in mother liquor containing 20% DMSO. Diffraction data were collected using a Rigaku MicroMax007 rotating anode source and a Rigaku Saturn92 CCD at 100 K. Data processing, data reduction and structure solution by molecular replacement were carried out using programs from the CCP4 suite.[13] (*S*)-**8b** was modeled into the electron density using AFITT and Coot.[14] The protein–compound complex model was refined using Refmac,[15] and the final structure[16] has been deposited in the Protein Data Bank with the deposition code 2w17 together with structure factors and detailed experimental conditions.
11. DeLano, W. L. The PyMOL molecular graphics system. DeLano Scientific, San Carlos, CA; 2003. Available from: http://www.pymol.org.
12. (a) Lawrie, A. M.; Noble, M. E.; Tunnah, P.; Brown, N. R.; Johnson, L. N.; Endicott, J. A. *Nat. Struct. Biol.* **1997**, *4*, 796; (b) Legraverend, M.; Tunnah, P.; Noble, M.; Ducrot, P.; Ludwig, O.; Grierson, D. S.; Leost, M.; Meijer, L.; Endicott, J. *J. Med. Chem.* **2000**, *43*, 1282.
13. CCP4 *Acta Crystallogr.* **1994**, *D50*, 760.
14. AFITT; Peat, T. S.; Christopher, J.; Schmidt, K. *Acta Crystallogr.* **2005**, *A61*, 165; Coot, ; Emsley, P.; Cowtan, K. *Acta Crystallogr.* **2004**, *D60*, 2126.
15. Refmac version 5.1.17, Murshudov, G. N.; Vagin, A. A.; Dodson, E. J. *Acta Crystallogr.* **1997**, *D53*, 240.
16. Crystallographic statistics for the CDK2-(*S*)-**8b** complex are as follows: space group $P2_12_12_1$, unit cell 53.542, 71.824, 71.771 Å, resolution 2.15 Å, 14,782 reflections from 51,812 observations give 99.7% completeness with R_{merge} of 9.5% and mean $I/\sigma(I)$ of 6.0. The final model containing 2209 protein, 154 water, and 33 compound atoms has an R-factor of 23.7% (R_{free} using 5% of the data 30.6%). Mean temperature factors for the protein and the ligand are 40.6 and 34.6 Å,[2] respectively.Compound (*S*)-**15b**: NMR (400 MHz, $CDCl_3$) δ 8.30 (d, 1H), 7.61–7.58 (m, 3H), 7.54 (d, 2H), 7.22 (s, 1H), 5.58 (septet, 1H), 3.89–3.63 (m, 2H), 3.58–3.20 (m, 3H), 2.62 (s, 3H), 2.48–2.39 (m, 3H), 2.23–1.96 (m, 1H), 1.84–1.74 (m, 1H), 1.53 (d, 6H); LCMS MH^+ 438.